PROCEEDINGS OF SCIENCE

Beyond the electroquenched approximation

Tim Harris

Institut für Theoretische Physik, ETH Zürich,
Wolfgang-Pauli-Str. 27, 8093 Zürich, Switzerland

E-mail: harrist@phys.ethz.ch

Lattice QCD determinations of hadronic matrix elements required for precision tests of the Standard Model are now approaching an accuracy where the electromagnetic interactions of the quarks can no longer be neglected. In particular, the electric charge of the sea quarks cannot be ignored a priori without introducing an uncontrolled systematic uncertainty. I review some of the challenges encountered in going beyond the electroquenched approximation, either when the QED effects are included via reweighting à la RM123 or when they are included directly in the importance sampling.

European network for Particle physics, Lattice field theory and Extreme computing (EuroPLEx2023)
11-15 September 2023
Berlin, Germany

PoS(EuroPLEx2023)011

1. Introduction

Lattice QCD predictions are reaching a level of sophistication where it is possible to provide reliable input for precision tests of the Standard Model, for example the fundamental parameters of QCD or low-energy hadronic matrix elements [1]. The achievable accuracy will be eventually limited by the omission of the electromagnetic interactions of the quarks, which break the isospin symmetry between up and down quarks, required to match Nature.

One prominent example where an accuracy of 1% or less has been claimed is the hadronic vacuum polarization contribution to the anomalous magnetic moment of the muon, and in particular the contribution from intermediate separations between the quark electromagnetic currents [2–11]. As illustrated in Fig. 1 (left), the isovector channel contribution has received much attention, while only a few predictions exist which include isospin-breaking effects (right) that can be independently compared with phenomenology [12] (blue). Scrutinizing further these predictions, only the computation of the BMW collaboration [2] (filled square) includes full estimates for isospin-breaking effects due to the sea quarks, which however rely on smaller lattice resolutions, smaller physical lattice extents and simulations with heavier quarks than used in the isovector contribution.

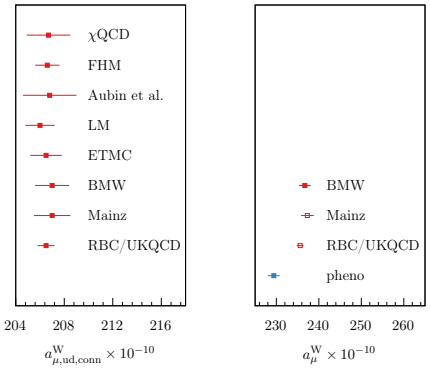

Figure 1: Recent lattice computations of the hadronic vacuum polarization contribution to the muon anomaly from intermediate separations. The left panel shows the many lattice QCD estimates performed of the isovector channel, while the right shows contributions including isospin-breaking effects which can be compared with phenomenological estimates.

The omission of such effects is sometimes called the electroquenched approximation which is essentially uncontrolled (see FLAG Sec. 3.1.2 [1]), although the BMW computation suggests the effects may be small in their chosen scheme. In the following section, we attempt to recap some of the hurdles to include the sea-quark effects which arise when reweighting from a theory defined with neutral quarks, postponing the discussion of QED in a finite volume until later. Afterwards, I provide a short update on the status of QCD+QED with $C^\star$ boundary conditions, which is a local and gauge-invariant finite-volume formulation used by the RC* collaboration.

2. Sea-quark effects in the RM123 method

One appealing approach to include the isospin-breaking effects is to note that given a sample distributed according to an action S_{QCD}, which describes a theory of neutral quarks with isospin

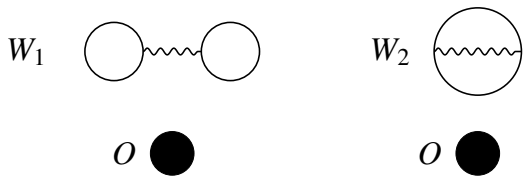

Figure 2: Wick contractions which contribute to Eq. (5)

symmetry, reweighting in the bare parameters, including to non-zero electric charge, allows one to re-use effectively existing gauge-field configurations [13]. Expanding the difference of the action to the full QCD+QED theory S in the differences of the bare parameters

$$S - S_{\rm QCD} = \delta\beta \frac{\partial S}{\partial \beta} + e \frac{\partial S}{\partial e} + \delta m_f \frac{\partial S}{\partial m_f} + \dots \tag{1}$$

one can define unambiguously the leading-order isospin-breaking corrections à la RM123

$$\langle O \rangle - \langle O \rangle_{\rm QCD} = \tfrac{1}{2} e^2 \langle [\tfrac{\partial S}{\partial e}]^2 O \rangle_{\rm QCD,c} - \delta m_f \langle \tfrac{\partial S}{\partial m_f} O \rangle_{\rm QCD,c} - \delta\beta \langle \tfrac{\partial S}{\partial \beta} O \rangle_{\rm QCD,c} + \dots, \tag{2}$$

given a specific choice of the renormalization conditions for both QCD and QCD+QED [14]. Note that, depending on the discretization, other corrections may be required, for example to $c_{\rm SW}$ in the O(a)-improved Wilson theory. The connected correlation functions required, for example

$$\langle [\tfrac{\partial S}{\partial e}]^2 O \rangle_{\rm QCD,c} = (-{\rm i})^2 \int_{x,y} \langle J_\mu(x) \overbrace{A_\mu(x) J_\nu(y) A_\nu}(y) O \rangle_{\rm QCD,c} \tag{3}$$

involve insertions of local operators like the electromagnetic current (here in continuum form)

$$J_\mu = \tfrac{2}{3} \bar{u} \gamma_\mu u - \tfrac{1}{3} \bar{d} \gamma_\mu d - \tfrac{1}{3} \bar{s} \gamma_\mu s + \tfrac{2}{3} \bar{c} \gamma_\mu c, \tag{4}$$

and the electromagnetic gauge potential $A_\mu(x)$.

In the simplest case of an observable O constructed from a product of neutral fields, for example the flowed gluonic energy density which defines the low-energy scale t_0 [15], the only Wick contractions which contribute to the correlation function Eq. (3)

$$W_{1,2} = -a^8 \sum_{x,y} H^{1,2}_{\mu\nu}(x,y) G_{\mu\nu}(x-y). \tag{5}$$

where $G_{\mu\nu}(x-y) = \overbrace{A_\mu(x) A_\nu}(y)$ is the gauge-fixed position-space photon propagator and $H^{1,2}$ are the traces of quark propagators $S^f = D_f^{-1}$

$$H^1_{\mu\nu}(x,y) = \textstyle\sum_{f,g} Q_f Q_g \, {\rm tr}\{\gamma_\mu S^f(x,x)\} \, {\rm tr}\{\gamma_\nu S^g(y,y)\}, \tag{6}$$

$$H^2_{\mu\nu}(x,y) = -\textstyle\sum_f Q_f^2 \, {\rm tr}\{\gamma_\mu S^f(x,y) \gamma_\nu S^f(y,x)\}, \tag{7}$$

depicted in Fig. 2. As we shall see, the computation of such classes of diagrams proves computationally demanding, which explains the slow progress in fully including their estimates in computations such as those described in the previous section.

2.1 Scaling of the statistical uncertainty

When all the diagrams are included and the lines of constant physics properly defined, the observations lead to finite unambiguous results in the continuum limit. Unfortunately, this does not guarantee the same behaviour for the statistical uncertainty, which hinders the removal of systematic effects due to the finite lattice spacing and volume. Following the lines of Ref. [16], the variance of the connected correlator Eq. (5) involving $O = O(z_1, z_2, \ldots)$ is dominated by vacuum contributions when when x, y are far from $z_1, z_2, \ldots$ and factorizes

$$\sigma^2 = \langle O^2 \rangle_{\mathrm{QCD,c}} \langle W_i^2 \rangle_{\mathrm{QCD,c}} + \ldots \tag{8}$$

$$= \sigma_O^2 \sigma_{W_i}^2 + \ldots \tag{9}$$

where $\sigma_{W_i}^2$ is the variance of the corresponding Wick contraction. This factorization has been shown to work out fairly well in simulations involving domain-wall and Wilson fermions. Such vacuum contributions contain the worst short-distance singularities of the total variance, whose leading behaviour in this case can be worked out by power counting

$$\sigma_{W_i}^2 \sim (L/a)^4, \tag{10}$$

where a is the lattice spacing. This contribution also exhibits the generic pathological behaviour of the variance with the lattice extent L when the vertices in the Wick contraction are integrated over the entire volume. Thus, the vertices of the insertions x, y should be restricted to the vicinity of the operator $z_1, z_2, \ldots$ as the volume is increased.

2.2 Estimating the volume sums

Evaluating the sums in Eq. (5) is not a straightforward task without introducing new sources of fluctuations. Simple implementations might involve uniform sampling of the coordinates of the vertices, or introducing stochastic estimates of both the hadronic traces and the electromagnetic potential. The extra noise introduced has the same short-distance structure as above, and can be even more significant, having tree-level contributions.

It may be possible to do better in certain cases by noting a few special properties of the Wick contractions which appear in Eq. (5) and avoid introducing a stochastic representation of the gauge potential. For Wilson-like or domain-wall fermions, due to the charge factors and isospin-symmetry of the QCD theory, it is possible to estimate the contributions of u, d, s quarks together in a single estimator for the traces, similar to the one-end trick of twisted-mass Wilson fermions [17], called the split-even estimator [16, 18]

$$\mathcal{T}_\mu(x) = \tfrac{1}{3}(m_\mathrm{s} - m_\mathrm{ud}) \frac{1}{N_\mathrm{s}} \sum_{i=1}^{N_\mathrm{s}} \{\eta_i^\dagger S_\mathrm{s}\}(x) \gamma_\mu \{S_\mathrm{ud} \eta_i\}(x), \tag{11}$$

where the auxiliary quark fields $\eta_i(x)$ have zero mean and finite variance. Thanks to the factorization of the traces, a stochastic estimator for the diagram $\mathcal{W}_1$ can be computed

$$\mathcal{W}_1 \approx \Big(a^4 \sum_x \mathcal{T}_\mu(x)\Big)\Big(a^4 \sum_y \mathcal{T}_\nu(y) G_{\mu\nu}(x-y)\Big), \tag{12}$$

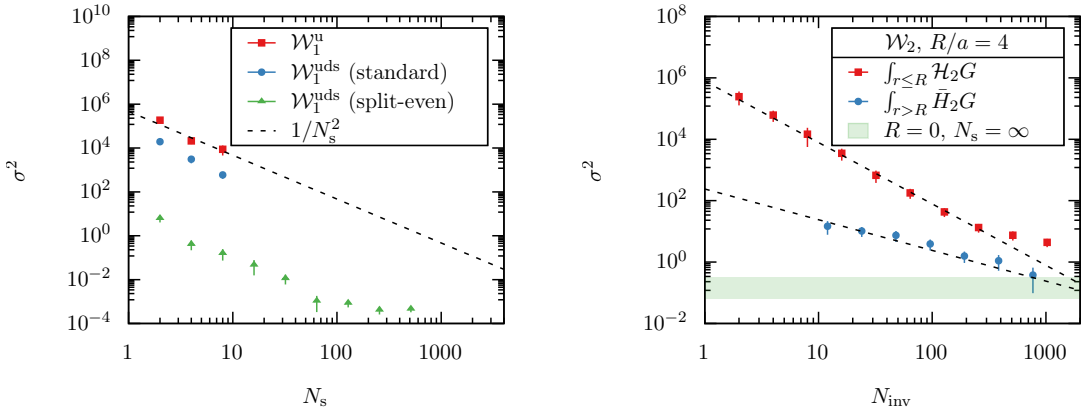

Figure 3: Left: Comparison of the variance versus the number of sources for the W_1 quark-line disconnected diagram, using a single flavour (red squares), the standard estimator for u, d, s flavours (blue circles) and the split-even estimator (green triangles). Right: the variances of the short-distance (red) and long-distance (blue) contributions to the estimator for the W_2 quark-line connected diagram.

where the second convolution can be computed efficiently using the Fast Fourier Transform.

On the other hand, the quark-line connected Wick contraction does not benefit from any cancellations between the flavour contributions. Motivated by the dominance of the short-distance contribution, it may be useful to decompose the diagram into its short and long distance contributions

$$\mathcal{W}_2 = a^4 \sum_{|r|\le R} \mathcal{H}^2_{\mu\nu}(r) G_{\mu\nu}(r) + a^4 \sum_{r>R} \bar{H}^2_{\mu\nu}(r) G_{\mu\nu}(r). \tag{13}$$

For small R the hadronic trace can be efficiently estimated stochastically, while the small remainder can be estimated using a small sample of base coordinates (point sources) distributed uniformly over the lattice, see Ref. [18] for details.

The estimators $\mathcal{W}_{1,2}$ were investigated using Shamir domain-wall fermions on a coarse $L/a = 24$ lattice with a pion mass of $m_\pi \approx 340\,\mathrm{MeV}$ and extent $m_\pi L \approx 4.9$ [18]. In Fig. 3 (left) the variance of $\mathcal{W}_1$ is shown as a function of the number of auxiliary field samples N_{s}, illustrating the expected leading scaling with $1/N_{\mathrm{s}}^2$. Three variants are shown, the variance of a single light flavour (red), of the up, down and strange quarks with a simple estimator (blue) and the split-even estimator (green). The last variant has much suppressed fluctuations due to the auxiliary fields, and reaches the gauge noise with a few hundred sources. The right-hand plot shows the variances of the short-distance (red) and long-distance (blue) contributions to $\mathcal{W}_2$ for a choice $R/a = 4$. As before, the stochastic estimator has an improved scaling in the variance $1/N_{\mathrm{s}}^2$ compared with the position-space method. The green band depicts an estimate of the gauge noise of the contact term, suggesting that the gauge noise can be reached with around a thousand inversions. At least it seems that some variance reduction methods may be useful to estimate precisely such contributions. Given that the fluctuations have a very different origin than those afflicting long distances in hadronic correlation functions, some thought may be required here.

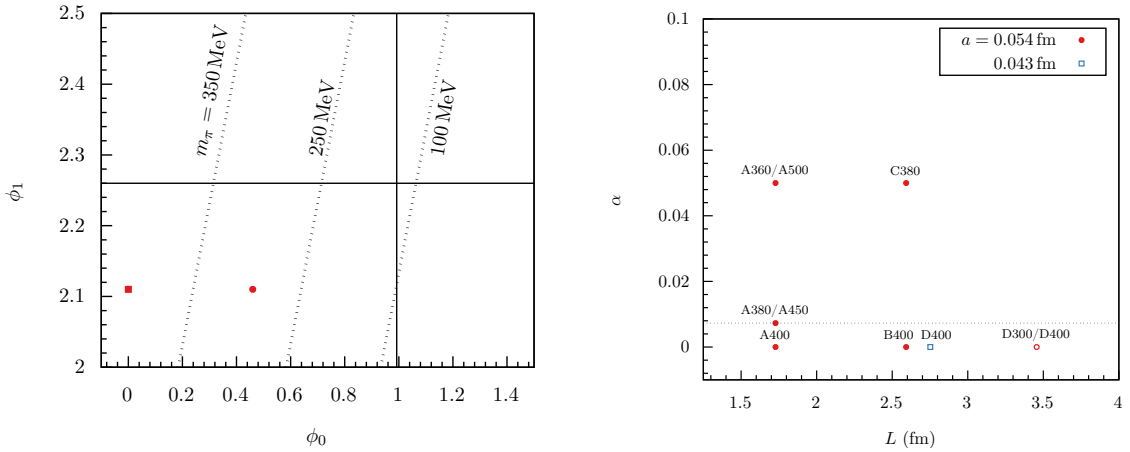

Figure 4: Left: the current lines of constant physics in the ϕ_0, ϕ_1 plane of the RC* simulations. The solid lines represent the physical values. Right: the simulation landscape in the plane of the electromagnetic coupling α and the lattice extent L. Open circles represent ongoing simulations.

3. QCD+QED with $C^\star$ boundary conditions

Lattice gauge theory simulations proceed necessarily in a finite volume, and periodic boundary conditions pose a barrier to the definition of electrically-charged states which are forbidden by Gauss's law. One way to circumvent the issue is to break the continuous global symmetry giving rise to the definition of the charge, which can be done softly by a judicious choice of the boundary conditions. The RC* collaboration has advocated the use of $C^\star$ or C-periodic boundary conditions [19]

$$A_\mu(x+L) = -A_\mu(x), \qquad \psi(x+L) = C^{-1}\psi^\top(x), \tag{14}$$

$$U_\mu(x+L) = U^\star_\mu(x), \qquad \bar\psi(x+L) = -\psi^\top(x)C, \tag{15}$$

which break the global U(1) symmetry down to a discrete subgroup, so that the charge (and, in fact all flavour) quantum numbers are only defined mod 2 [20]. In QCD+QED the effects of flavour-symmetry breaking are exponentially suppressed in the lattice extent, so this formulation results in a practical way to compute the properties of charged hadrons while preserving gauge-invariance, locality and translation invariance. While the boundary conditions impose some extra technical challenges, such as the sampling of the Pfaffian of the Dirac operator which involves rational approximations [21], reduced finite-volume effects in this formulation are expected to ameliorate any extra cost [22, 23].

The collaboration has initiated a large-scale simulation programme to investigate QCD+QED with $C^\star$ boundary conditions using both the RM123 method and sampling directly the joint distribution [22]. With four flavours, the theory requires the imposition of six renormalization conditions to fix the bare parameters of the couplings α, β and the quark masses $m_\mathrm{u}, m_\mathrm{d}, m_\mathrm{s}, m_\mathrm{c}$, which is done by setting the following hadronic masses

$$\phi_0 = 8t_0(M^2_{K^\pm} - M^2_{\pi^\pm}), \qquad \phi_1 = 8t_0(M^2_{K^\pm} + M^2_{\pi^\pm} + M^2_{K^0}), \tag{16}$$

$$\phi_2 = 8t_0(M^2_{K^0} - M^2_{K^\pm})/\alpha_\mathrm{R}, \qquad \phi_3 = \sqrt{8t_0}(M_{D_\mathrm{s}^\pm} + M_{D^0} + M_{D^\pm}), \tag{17}$$

as well as the gradient-flow scale $\sqrt{8t_0}$ and the renormalized electromagnetic coupling α_{R} to some prescribed values. The main line of constant physics is defined by the following unphysical choice

$$\phi_0 = 0, \quad \phi_1 = 2.11, \quad \phi_2 = 2.36, \quad \phi_3 = 12.1, \quad \sqrt{8t_0} = 0.415\,\mathrm{fm} \tag{18}$$

for various values of α_{R}. The first condition is equivalent to setting $m_{\mathrm{d}} = m_{\mathrm{s}}$, which reduces the number of parameters needed to be tuned to three, as the last condition can be imposed freely for a given β and is equivalent to setting the scale. This choice is represented in the plane of ϕ_0, ϕ_1 by the square in Fig. 4 (left), where the solid lines represent the corresponding physical values.

Although the inclusion of the electromagnetic potenital is not especially computationally demanding, the non-perturbative tuning of the parameters is a formidable task [24–26]. The tuning has been accomplished with the help of the computation of reweighting factors in the physics parameters, either by computing them non-perturbatively or expanding via the method of insertions as in the previous section. First efforts have also begun to simulate at non-zero ϕ_0 see the circle in Fig. 4 (left), which represents an important step toward physical quark masses.

In the right-hand panel, the simulation landscape is illustrated in the plane of bare coupling α and lattice extent L. These simulations have already been used to investigate isospin-breaking effects in a number of interesting observables such as the hadronic spectrum [22, 27] and the electromagnetic current correlator [28, 29]. Crucial to the success of this program is the implementation of modern variance-reduction techniques [30, 31]. In the near future, these simulations will also allow us to test empirically our expectations about finite-volume effects with $C^\star$ boundary conditions [23] and the scaling of the uncertainty with the lattice parameters. New simulations at finer lattice spacing and larger volumes (open symbols in Fig. 4, right) will serve to control systematic effects and allow the collaboration to extend the physics reach of the program to new observables.

4. Conclusion

Lattice QCD computations of isospin-breaking effects are advancing rapidly, driven by the need for accurate unambiguous predictions from the Standard Model. For the most part, the sea-quark effects have been neglected until now, due to their computational complexity, which I attempted to shed some light upon here. To avoid any uncontrolled uncertainties, however, these effects must be included, either via reweighting and the method of operator insertions or via direct sampling. If QED is to be included in a finite volume, then special care is required about its formulation, for example via $C^\star$ boundary conditions as advocated by the RC* collaboration. The simulation program of the collaboration is progressing steadily, and one important ongoing activity is to compare quantitatively the cost of implementing QCD+QED via the RM123 method or non-perturbatively by sampling the joint distribution.

Acknowledgements The author would like to thank the members of the RC* collaboration for useful discussions.

References

[1] Y. Aoki et al. In: *Eur. Phys. J. C* 82.10 (2022), p. 869. arXiv: 2111.09849 [hep-lat].

[2] S. Borsanyi et al. In: *Nature* 593.7857 (2021), pp. 51–55. arXiv: 2002.12347 [hep-lat].

[3] C. Alexandrou et al. In: *Phys. Rev. D* 107.7 (2023), p. 074506. arXiv: 2206.15084 [hep-lat].

[4] A. Bazavov et al. In: *Phys. Rev. D* 107.11 (2023), p. 114514. arXiv: 2301.08274 [hep-lat].

[5] G. Wang et al. In: *Phys. Rev. D* 107.3 (2023), p. 034513. arXiv: 2204.01280 [hep-lat].

[6] T. Blum et al. In: *Phys. Rev. D* 108.5 (2023), p. 054507. arXiv: 2301.08696 [hep-lat].

[7] M. Cè et al. In: *Phys. Rev. D* 106.11 (2022), p. 114502. arXiv: 2206.06582 [hep-lat].

[8] C. Aubin et al. In: *Phys. Rev. D* 106.5 (2022), p. 054503. arXiv: 2204.12256 [hep-lat].

[9] C. Lehner and A. S. Meyer. In: *Phys. Rev. D* 101 (2020), p. 074515. arXiv: 2003.04177 [hep-lat].

[10] A. Gérardin et al. In: *Phys. Rev. D* 100.1 (2019), p. 014510. arXiv: 1904.03120 [hep-lat].

[11] T. Blum et al. In: *Phys. Rev. Lett.* 121.2 (2018), p. 022003. arXiv: 1801.07224 [hep-lat].

[12] G. Colangelo et al. In: *Phys. Lett. B* 833 (2022), p. 137313. arXiv: 2205.12963 [hep-ph].

[13] G. M. de Divitiis et al. In: (Feb. 2012). arXiv: 1202.5222 [hep-lat].

[14] G. M. de Divitiis et al. In: *Phys. Rev. D* 87.11 (2013), p. 114505. arXiv: 1303.4896 [hep-lat].

[15] M. Lüscher. In: *JHEP* 08 (2010). [Erratum: JHEP 03, 092 (2014)], p. 071. arXiv: 1006.4518 [hep-lat].

[16] L. Giusti et al. In: *Eur. Phys. J. C* 79.7 (2019), p. 586. arXiv: 1903.10447 [hep-lat].

[17] P. Boucaud et al. In: *Comput. Phys. Commun.* 179 (2008), pp. 695–715. arXiv: 0803.0224 [hep-lat].

[18] T. Harris et al. In: *PoS* LATTICE2022 (2023), p. 013. arXiv: 2301.03995 [hep-lat].

[19] A. S. Kronfeld and U. J. Wiese. In: *Nucl. Phys. B* 357 (1991), pp. 521–533.

[20] B. Lucini et al. In: *JHEP* 02 (2016), p. 076. arXiv: 1509.01636 [hep-th].

[21] J. Lücke. PhD thesis. Humboldt U., Berlin, 2024.

[22] L. Bushnaq et al. In: *JHEP* 03 (2023), p. 012. arXiv: 2209.13183 [hep-lat].

[23] S. Martins and A. Patella. In: *PoS* LATTICE2022 (2023), p. 323. arXiv: 2212.09565 [hep-lat].

[24] A. Altherr et al. In: *PoS* LATTICE2022 (2023), p. 259. arXiv: 2212.10894 [hep-lat].

[25] J. Lücke et al. In: *PoS* LATTICE2022 (2023), p. 064. arXiv: 2212.09578 [hep-lat].

[26] R. Höllwieser et al. In: *Eur. Phys. J. C* 80.4 (2020), p. 349. arXiv: 2002.02866 [hep-lat].

[27] M. Hansen et al. In: *JHEP* 05 (2018), p. 146. arXiv: 1802.05474 [hep-lat].

[28] A. Altherr et al. In: *PoS* LATTICE2022 (2023), p. 312. arXiv: 2212.11551 [hep-lat].

[29] A. Altherr et al. In: *PoS* LATTICE2022 (2023), p. 281. arXiv: 2301.04385 [hep-lat].

[30] A. Cotellucci and A. Patella. In: *PoS* LATTICE2023 (2024), p. 002. arXiv: 2312.08972 [hep-lat].

[31] R. Gruber et al. In: (Jan. 2024). arXiv: 2401.14724 [hep-lat].